Mendeleev Communications

Mendeleev Commun., 2025, **35**, 487–489

Halloysite nanotubes as an effective adsorbent of chlorhexidine acetate

Olga V. Alekseeva, Andrew V. Noskov,* Daria N. Yashkova and Alexander V. Agafonov

G. A. Krestov Institute of Solution Chemistry, Russian Academy of Sciences, 153045 Ivanovo, Russian Federation. E-mail: avn@isc-ras.ru

DOI: 10.71267/mencom.7721

New composite antimicrobial materials based on halloysite and the antiseptic drug chlorhexidine acetate have been synthesized and studied *via* the adsorption method. During the drug adsorption, both the surface area and the pore space volume decrease due to the filling of the halloysite pores. For the first time, the density functional method has been used to assess the differences in the texture of the studied materials.

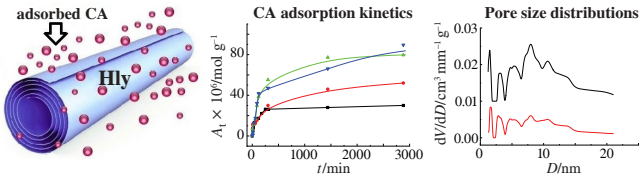

Keywords: halloysite, chlorhexidine acetate, adsorption, porosity, antimicrobial properties.

Composite materials based on non-toxic, eco-friendly and inexpensive natural clay minerals are widely used in nanotechnology, medicine pharmacy, cosmetics and ecological applications.[1–3] Currently, special attention is being paid to halloysite (Hly), a clay mineral consisting of multilayer aluminosilicate nanotubes possessing a cavity inside. The tubes are formed by a rolled aluminosilicate sheet, its elementary layer has a 1 : 1 structure and contains the tetrahedral silicon–oxygen and octahedral aluminohydroxyl networks.[4,5] The length of the halloysite nanotubes is 500–1500 nm, the outer diameter is 50–80 nm and the inner diameter is 10–15 nm.

There are earlier studies on the use of halloysite as a promising drug delivery system, catalyst, an adsorbent for metal ions and organic compounds and polymer fillers.[6–12] Various antiseptics (chlorhexidine, povidone–iodine, brilliant green and iodine) and antibiotics (tetracycline, gentamicin, doxycycline, amoxicillin and ciprofloxacin) loaded into halloysite nanotubes are reported to be released within 5–10 h and to provide more effective elimination of the bacteria.[13,14]

Among the above antiseptic drugs, chlorhexidine is a broad-spectrum biocide effective against gram-positive and gram-negative bacteria and fungi. However, one of the challenges of using chlorhexidine in biomedicine is its low water solubility.[15] Therefore, in practice, chlorhexidine is used in the form of gluconate and acetate salts. Moreover, chlorhexidine acetate (CA) has lower solubility compared with chlorhexidine bigluconate.

Most of the works relate to the study of the physicochemical properties and biological activity of clay minerals intercalated with chlorhexidine gluconate, *e.g.*, an environmentally friendly antibacterial composite has been obtained by loading the natural halloysite nanotubes with chlorhexidine gluconate.[16] Based on the inhibition zone test results, the authors concluded that the prepared composite is a safe and promising antibacterial agent and it has a great potential for application in the textile field. Halloysite loaded with chlorhexidine digluconate and its dental applications have been also studied.[17,18] It was found that incorporation of halloysite/chlorhexidine materials in the dental resin composites has significantly improved their mechanical properties and ensured considerable antibacterial activity. It should be noted that in the above works, chlorhexidine immobilized in halloysite was obtained from non-aqueous (alcohol) solutions *via* the vacuum technology.

The data on the intercalation of chlorhexidine acetate into aluminosilicate-based matrices is very limited. In this regard, we aimed to study both the kinetics of sorption of the antiseptic preparation chlorhexidine acetate on halloysite nanotubes and the structure, morphology and antibacterial properties of the resulting composite material.

The composites synthesis was carried out in a simpler way than the one used in the early reports.[17,18] Specifically, we have loaded the CA into halloysite nanotubes by adsorption from aqueous medium. For this purpose, the aqueous CA solutions of concentrations (C_0) of 0.29×10^{-4}, 0.7×10^{-4}, 1.0×10^{-4} and 1.5×10^{-4} mol dm^{-3} were prepared at room temperature. Then, the weighted samples of the halloysite powder (0.005 g) were placed into the test tubes, mixed with 5 ml of aqueous solutions of CA of the listed concentrations, kept under stirring for a certain time, after which the phases were separated. The concentration of CA in the solution after adsorption was determined by spectrophotometric method. The amount of the adsorbed drug (A_t) was determined with consideration of the initial concentration in the solution, the volume of the test tube and the mass of the adsorbent sample.

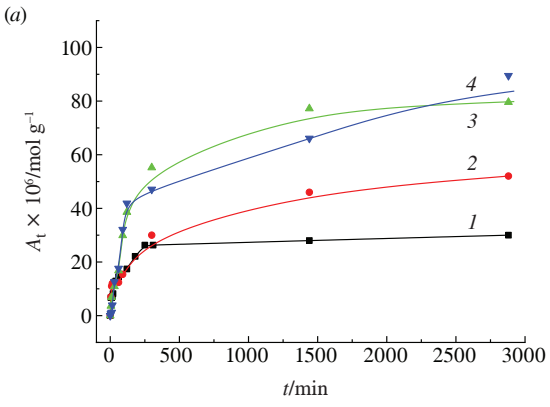

Figure 1 Effect of the initial CA concentration (C_0) on the drug amount adsorbed by halloysite. C_0 values: (*1*) 0.29×10^{-4}, (*2*) 0.7×10^{-4}, (*3*) 1.0×10^{-4} and (*4*) 1.5×10^{-4} mol dm^{-3}.

The results of the kinetic studies (see Figure 1) showed that the accumulation of the drug in the solid phase had occurred fast at first, then slow and then reached equilibrium. The adsorption equilibrium time ranged from 300 to 3000 min depending on the initial concentration.

The changes in the physicochemical characteristics of halloysite as a result of its saturation with chlorhexidine acetate during adsorption from the solution with an initial concentration of 1.5×10^{-4} mol dm^{-3} for 2880 min are described below.

To identify the chemical elements in the surface layer of halloysite before and after adsorption of the drug, the energy dispersive analysis (EDS) was used. In the EDS spectra of the studied materials, peaks of oxygen, aluminum and silicon characteristic of the original halloysite have been observed. In addition, the peaks of nitrogen and chlorine containing in CA, have appeared in the sample after the adsorption of CA.

The crystal structure of the materials under consideration was investigated *via* X-ray diffraction. Analysis of the obtained data allowed us to conclude that there are no significant differences between the XRD patterns for the pristine and CA-loaded halloysite. For example, for the pristine aluminosilicate, the basal distance d_{001} calculated for the main reflection (001) by the Bragg formula is 0.751 ± 0.010 nm, that deviates slightly from the value for Hly/CA (0.737 ± 0.011 nm). Thus, the process of CA loading does not change the crystal structure of halloysite. The similar conclusion has been made earlier for kaolinite,[19] which has a composition similar to halloysite, but a lower water content.

To assess changes in the porous structure of clay mineral due to CA loading, we used the low-temperature (77 K) nitrogen adsorption–desorption technique. It was found that the corresponding isotherms were characterized by the presence of capillary-condensation hysteresis loops, hence, the studied materials could be classified as mesoporous.

The textural parameter values for halloysite before and after CA adsorption were determined *via* the analysis of these isotherms using Brunauer–Emmett–Teller (BET), Barrett–Joyner–Halenda (BJH) and the density functional theory (DFT) methods.[20–22] The data obtained are presented in Table 1.

Here, S_{BET} and S_{BJH} represent the total surface area determined *via* BET and BJH models, respectively; V_{BJH} and V_{DFT} are the pore volumes determined *via* BJH and DFT methods, respectively; D_{av} is the average pore diameter determined *via* BJH method; D_{prob} is the most probable pore diameter coinciding with the maximum in the BJH pore size distribution.

The data presented in Table 1 show that for the Hly/CA sample, both the surface area (S_{BET} and S_{BJH} values) and the pore volume (V_{BJH} and V_{DFT} values) are significantly less than those for the pristine halloysite. It can be assumed that the porosity decreased, inasmuch as the halloysite lumen has been occupied with CA. The ability of filling is due to the fact that the pore sizes (Table 1) exceed the sizes of the CA molecule (0.5 nm). [23]

The data in Table 1 prove that mesopores of 7–15 nm in size (the peak at 8.8 nm), presented in halloysite, have not been detected in the Hly/CA sample. This may indicate that they are halloysite cavities filled with CA molecules. It should be noted that this assumption is in a good agreement with earlier results,[24] where a pore size distribution with the peaks at 3.5, 11 and 22 nm has been found for halloysite; the peaks at 11 and 22 nm have been identified as lumina in halloysite nanotubes.

Table 1 The porous parameter values for Hly and Hly/CA.

Sample	S_{BET}/ m^2 g^{-1}	S_{BJH}/ m^2 g^{-1}	V_{BJH}/ cm^3 g^{-1}	V_{DFT}/ cm^3 g^{-1}	D_{av}/ nm	D_{prob}/ nm
Hly	57.4	49.7	0.15	0.13	10.9	4.1 and 8.8
Hly/CA	34.7	25.5	0.08	0.06	9.3	4.0

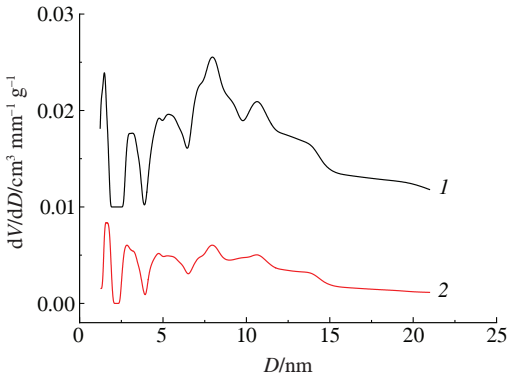

Figure 2 Pore size distributions plotted *via* the DFT model for (*1*) Hly and (*2*) Hly/CA samples.

It is also evident from Table 1 that the V_{BJH} and V_{DFT} values are different for both materials under study. Unlike the BJH model, the DFT method is based on the fundamental principle of the minimum of the thermodynamic functional and it can be used for both microporous and mesoporous samples. It provides a more reasoned and versatile approach to calculating the pore structure parameters than the conventional methods based on the Kelvin equation.[22] When applying this approach, the assumption is made that all pores have the same shape and differ only in characteristic sizes.

Figure 2 shows that in the pore size distribution determined by the DFT method, four groups of pores can be distinguished in the range of 0–10 nm. As can be seen, for samples of CA-loaded halloysite, the maxima corresponding to these groups are 3–5 times lower compared with those for the pristine halloysite. This also indicates that the clay material pores are filled with the drug. And besides, the volume occupied by the narrowest pores decreases less than others.

Given the obtained results, we can conclude that, due to its porous structure, the clay mineral halloysite is able to capture the chlorhexidine acetate molecules effectively. The adsorption level reached 98%, that demonstrated halloysite to be a potential adsorbent for removing antiseptic drugs from the liquid media.

The antibacterial activity of the original halloysite and halloysite saturated with chlorhexidine acetate was studied in relation to gram-negative bacteria *Escherichia coli*. The study was carried out using the generally accepted method – sowing 'lawn' in Petri dishes – using Endo nutrient medium. The test culture was evenly disposed over the surface of the nutrient medium, the studied samples of Hly and Hly/CA in the form of tablets were placed above and incubated in a thermostat at 37 °C for 24 h. The results obtained for cultivating bacteria in Endo medium in the absence of the studied samples were selected as controls.

Figure 3 shows photographs of the content of the Petri dishes after the removal of the Hly/CA samples, as well as the visual results of the control test. Comparison of the presented images reveals that the effect of the halloysite samples saturated with

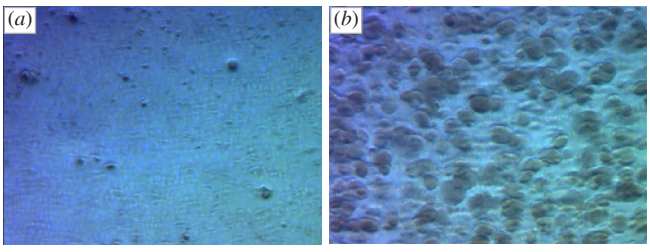

Figure 3 Photos demonstrating the viability of *E. coli* culture in Endo medium: (*a*) under Hly/CA sample and (*b*) control.

chlorhexidine acetate results in the significant decrease in the number of *E. coli* colonies inside the nutrient medium, *i.e.*, the antimicrobial effect of the material is detected. At the same time, it was found that in the case of using samples of the original halloysite, the visual results are practically the same as the control results.

It is noteworthy that similar conclusions have been made in the aforementioned work,[19] in which the emergence of antimicrobial properties for kaolinite modified with chlorhexidine acetate has been demonstrated by the diffusion disk method.

To conclude, the results of the present study may be used for the development of new types of nanocomposite materials with antibacterial activity.

This study was financed by the State Assignment (subject No. 122040500044-4). The measurements were performed in the Centre for joint use of scientific equipment 'The upper Volga region centre of physico-chemical research'.

Online Supplementary Materials

Supplementary data associated with this article can be found in the online version at doi: 10.71267/mencom.7721.

References

1 Z. R. Gatabi, N. Heshmati, M. Mirhoseini and M. Dabbaghianamiri, *Arabian J. Sci. Eng.*, 2023, **48**, 8481; https://doi.org/10.1007/s13369-022-06959-3.
2 O. V. Alekseeva, A. N. Rodionova, A. V. Noskov and A. V. Agafonov, *Clays Clay Miner.*, 2019, **67,** 471; https://doi.org/10.1007/s42860-019-00037-w.
3 M. Ahmed and A. Nasar, *Arabian J. Sci. Eng.*, 2024, **49**, 801; https://doi.org/10.1007/s13369-023-08518-w.
4 K. Tazaki, *Clays Clay Miner.*, 2005, **53**, 224; https://doi.org/10.l346/CCMN.2005.0530303.
5 M. N. Shipko, M. A. Stepovich, A. V. Noskov, O. V. Alekseeva and D. N. Smirnova, *Bull. Russ. Acad. Sci.: Phys.*, 2022, **86**, 1011; https://doi.org/10.3103/S1062873822090283.
6 Y. M. Lvov, D. G. Shchukin, H. Möehwald and R. R. Price, *ACS Nano*, 2008, **2**, 814; https://doi.org/10.1021/nn800259q.
7 A. Gładysz-Płaska, M. Majdan, B. Tarasiuk, D. Sternik and E. Grabias, *J. Hazard. Mater.*, 2018, **354**, 133; https://doi.org/10.1016/j.jhazmat.2018.03.057.
8 R. Liu, B. Zhang, D. Mei, H. Zhang and J. Liu, *Desalination*, 2011, **268**, 111; https://doi.org/10.1016/j.desal.2010.10.006.
9 M. Fizir, W. Liu, X. Tang, F. Wang and Y. Benmokadem, *Clays Clay Miner*., 2022, **70**, 660; https://doi.org/10.1007/s42860-022-00210-8.
10 H. Li, X. Zhu, H. Zhou and S. Zhong, *Colloids Surf., A*, 2015, **487**, 154; https://doi.org/10.1016/j.colsurfa.2015.09.062.
11 N. Q. Nguyen, Y. Jeong, L. Abelmann, J. Ryu and D. Sohn, *Colloids Surf., A*, 2024, **680**, 132631; https://doi.org/10.1016/j.colsurfa.2023.132631.
12 F. Jaberifard, N. Arsalani, M. Ghorbani and H. Mostafavi, *Colloids Surf., A*, 2022, **637**, 128122; https://doi.org/10.1016/j.colsurfa.2021.128122.
13 Y. Lvov, W. Wang, L. Zhang and R. Fakhrullin, *Adv. Mater*., 2016, **28**, 1227; https://doi.org/10.1002/adma.201502341.
14 W. Wei, R. Minullina, E. Abdullayev, R. Fakhrullin, D. Mills and Y. Lvov, *RCS Adv*., 2014, **4**, 488; https://doi.org/10.1039/c3ra45011b.
15 X. Feng, A. Farajtabar, H. Lin, G. Chen, Y. He, X. Li and H. Zhao, *J. Chem. Thermodyn.*, 2019, **129**, 148; https://doi.org/10.1016/j.jct.2018.09.008.
16 Y. Wu, Y. Yang, H. Liu, X. Yao, F. Leng, Y. Chen and W. Tian, *RSC Adv*., 2017, **7**, 18917; https://doi.org/10.1039/c7ra01464c.
17 T. Barot, D. Rawtani and P. Kulkarni, *J. Compos. Sci.*, 2020, **4**, 81; https://doi.org/10.3390/jcs4020081.
18 S. Kalagi, S. A. Feitosa, E. A. Münchow, V. M. Martins, A. E. Karczewski, N. B. Cook, K. Diefenderfer, G. J. Eckert, S. Geraldeli and M. C. Bottino, *Dent. Mater*., 2020, **36**, 687; https://doi.org/10.1016/j.dental.2020.03.007.
19 S. K Jou and N. A. N. N. Malek, *Appl. Clay Sci*., 2016, **127**–**128**, 1; https://doi.org/10.1016/j.clay.2016.04.001.
20 K. S. W. Sing, *Adv. Colloid Interface Sci.*, 1998, **76**–**77**, 3; https://doi.org/10.1016/S0001-8686(98)00038-4.
21 K. K. Aligizaki, *Pore Structure of Cement-Based Materials: Testing Interpretation and Requirements*, 1st edn., CRC Press, New York, 2004; https://doi.org/10.1201/9781482271959.
22 J. Landers, G. Yu. Gor and A. V. Neimark, *Colloids Surf., A*, 2013, **437**, 3; https://doi.org/10.1016/j.colsurfa.2013.01.007.
23 B. Sun, M. Zhang, N. Zhou, X. Chu, P. Yuan, C. Chi, W. Fan and J. Shen, *RSC Adv*., 2018, **8**, 21369; https://doi.org/10.1039/C8RA03651A.
24 D. Tan, P. Yuan, F. Annabi-Bergaya, H. Yu, D. Liu, H. Liu and H. He, *Microporous Mesoporous Mater.*, 2013, **179**, 89; https://doi.org/10.1016/j.micromeso.2013.05.007.

Received: 9th January 2025; Com. 25/7721